Diaphyseal bone formation in murine tibiae in response to knee loading

Ping Zhang, Shigeo M. Tanaka, Hui Jiang, Min Su and Hiroki Yokota

J Appl Physiol 100:1452-1459, 2006. First published 12 January 2006;
doi: 10.1152/japplphysiol.00997.2005

Journal of Applied Physiology publishes original papers that deal with diverse area of research in applied physiology, especially those papers emphasizing adaptive and integrative mechanisms. It is published 12 times a year (monthly) by the American Physiological Society, 9650 Rockville Pike, Bethesda MD 20814-3991. ISSN: 8750-7587, ESSN: 1522-1601. Visit our website at http://www.the-aps.org/.

J Appl Physiol 100: 1452–1459, 2006.
First published January 12, 2006; doi:10.1152/japplphysiol.00997.2005.

Diaphyseal bone formation in murine tibiae in response to knee loading

Ping Zhang,[1] Shigeo M. Tanaka,[2] Hui Jiang,[3] Min Su,[1] and Hiroki Yokota[1,3]

[1]*Departments of Anatomy and Cell Biology, and* [3]*Biomedical Engineering, Indiana University-Purdue University Indianapolis, Indianapolis, Indiana; and* [2]*Graduate School of Natural Science and Technology, Kanazawa University, Ishikawa, Japan*

Submitted 18 August 2005; accepted in final form 30 December 2005

Zhang, Ping, Shigeo M. Tanaka, Hui Jiang, Min Su, and Hiroki Yokota. Diaphyseal bone formation in murine tibiae in response to knee loading. *J Appl Physiol* 100: 1452–1459, 2006. First published January 12, 2006; doi:10.1152/japplphysiol.00997.2005.—Mechanical stimulation is critical for bone architecture and bone mass. The aim of this study was to examine the effects of mechanical loads applied to the knee. The specific question was whether loads applied to the tibial epiphysis would enhance bone formation in the tibial diaphysis. In C57/BL/6 mice, loads of 0.5 N were applied for 3 min per day for 3 days at 5, 10, or 15 Hz. Bone samples were harvested 13 days after the last loading. The strains were measured 13 ± 2 μstrains at 5 Hz in the diaphysis. The histomorphometric data in the diaphysis clearly showed enhanced bone formation. First, compared with nonloaded control the cross-sectional cortical area was increased by 11% at 5 Hz and 8% at 10 Hz (both $P < 0.05$). Second, the cortical thickness was elevated by 12% at 5 Hz ($P < 0.01$) and 8% at 10 Hz ($P < 0.05$). Third, mineralizing surface (MS/BS), mineral apposition rate (MAR), and bone formation rate (BFR/BS) were increased at 5 Hz ($P < 0.01$ for MS/BS; $P < 0.001$ for MAR and BFR/BS) and at 10 Hz ($P < 0.05$ for MS/BS; $P < 0.01$ for MAR and BFR/BS). Bone formation was enhanced more extensively in the medial side than the lateral or the posterior side. The results reveal that knee loading is an effective means to enhance bone formation in the tibial diaphysis in a loading-frequency dependent manner without inducing significant in situ strain at the site of bone formation.

mechanical loading of bone; mouse; tibial diaphysis

BONE IS A MECHANOSENSITIVE tissue that adapts its mass, architecture, and mechanical properties to external loading. Various loading modalities have been developed to enhance bone formation including axial loading (33), four-point bending (11, 15), and high-frequency vibration (20, 22). Although the exact mechanisms for load-driven bone formation are still under investigation and the mechanism with the axial ulna loading (33), for instance, can be different from the mechanism with high-frequency vibrations (16), many studies indicate a role for strain and intramedullary pressure. There is a growing body of evidence demonstrating that interstitial fluid flow induced by strain and/or a pressure gradient plays a key role in enhancement of bone formation (3, 12, 16, 24). Interstitial fluid flow in cortical bone was monitored by using dye migration in a histological section (30), and recently a "fluorescence after photo-bleaching" technique was applied to evaluate load-driven flow phenomena in a lacunocanalicular network (9, 14, 23, 32). It is conceivable, for instance, that in situ strain induces interstitial fluid flow and enhances bone formation (2, 5, 31). Although the strain requirement differs among loading frequencies and target bones, osteogenic potentials at the site of unstrained bone are largely unexplored. In this report, we address the question of whether bone formation is stimulated in nonstrained diaphyseal bone by loads that are remotely applied to epiphyseal bone.

To answer that question, a novel mechanical loading model, "knee-loading modality," was developed and a custom-made piezoelectric mechanical loader was fabricated. Our hypothesis was that knee loading is effective in enhancing diaphyseal bone formation in tibiae in a loading frequency-dependent manner. In knee loading, mechanical loads are applied to the epiphysis of a proximal tibia as well as a distal femur. These epiphyses are directly under stress, but cortical bone in the diaphysis is distant from the loading site and not directly loaded. Unlike the ulna-loading modality or the tibia four-point bending modality, the knee-loading modality is therefore not aimed to induce strain in the diaphysis, a potential site of bone formation in this study. Instead, the rationale is to stimulate bone formation in the unstrained diaphyseal bone through remote strain in the epiphyseal bone at the loading site. Our previous studies showed osteogenic potentials in the ulna with the elbow-loading modality (25, 34), and the present study is designed to examine new bone formation in the tibia with the knee-loading modality.

In this study the piezoelectric mechanical loader previously employed for the elbow-loading modality was used for the knee-loading modality. It allowed us to apply a precise amount of loads at varying frequency. Many previous studies indicated dependence of bone remodeling on loading frequencies (26, 28, 33), and here we examined the effects of knee loading with a sinusoidal waveform at 5, 10, and 15 Hz. To evaluate in situ strain at the site of bone formation, we measured strains using strain gauges. The results of bone histomorphological analyses reveal that the knee-loading modality can induce load-driven bone formation in a loading-frequency-dependent manner at the site with virtually no in situ strain.

MATERIALS AND METHODS

Animal preparation. Twenty-eight female C57/BL/6 mice, ~14 wk of age (~20 g body wt), were used (Harlan-Sprague-Dawley, Indianapolis, IN). Four to five mice were housed per cage at the Laboratory Animal Resource Center of Indiana University, and they were fed with mice chow and water ad libitum. The animals were allowed to acclimate for 2 wk before the experiment. All procedures performed in this study were in accordance with guidelines of the Institutional Animal Care and Use Committee, which approved the protocol.

Mechanical loading. The mouse was placed in an anesthetic induction-chamber to induce sedation and mask anesthetized using 2% isoflurane. Mechanical loads were applied with the piezoelectric

Address for reprint requests and other correspondence: H. Yokota, Dept. of Biomedical Engineering, Indiana Univ.-Purdue Univ. Indianapolis, 723 West Michigan St., Indianapolis, IN 46202 (e-mail: hyokota@iupui.edu).

The costs of publication of this article were defrayed in part by the payment of page charges. The article must therefore be hereby marked "*advertisement*" in accordance with 18 U.S.C. Section 1734 solely to indicate this fact.

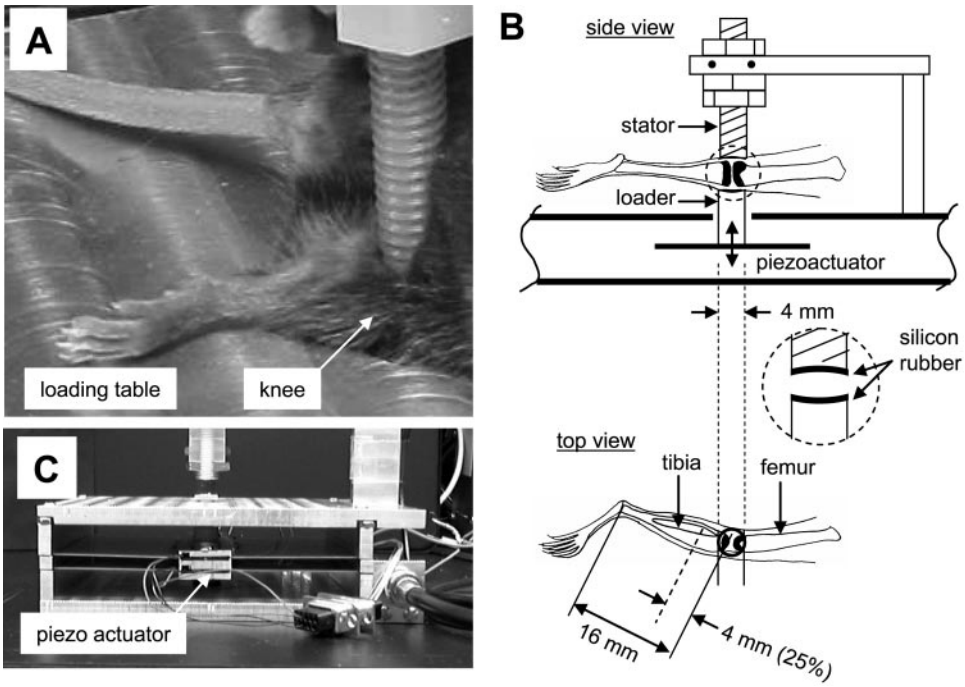

Fig. 1. Piezoelectric mechanical device used in this study. *A*: mouse on a loading table for the knee-loading modality (mask anesthesia is not shown for clarity). *B*: schematic diagram illustrating the loading site. The knee is placed between the stator and the loader, which is driven by a piezoelectric actuator. The loader is 4 mm in diameter, and the typical tibia is 16 mm in length (~14 wk, ~20 g). Load-driven bone formation was examined at the cross section ~4 mm (25%) distant from the proximal end of the tibia. *C*: side view of a piezoelectric actuator.

loader for 3 min per day for 3 consecutive days to the left knee (Fig. 1). The lateral and the medial sides of the tibia were in contact to the loader and the stator, respectively. To position the knee properly for the loading experiment, the lower end of the loading rod and the upper end of the supporter (nylon screw) were designed to form a pair of semispherical cups. The lateral and medial condyles of the tibia together with the medial and lateral epicondyles of the femur were confined in the cups. The tip of the loader had a contact area of 4 mm in diameter. To avoid a local stress concentration between the knee and the loader, both the loading surface and supporter were covered with silicon rubber. The mice were randomly divided into three groups for three loading frequencies (5, 10, or 15 Hz, $n = 8$), and loading with a peak-to-peak force of 0.5 N was applied to a left knee in the lateral-medial direction.

The applied force was calibrated by using a strain gauge on the aluminum cantilever connected to the stator. Note that force calibration was conducted in the same configuration to the loading experiment to an anesthetized animal, and an intact mouse leg was placed between the stator and the loader. In knee loading, the calibrated force of 0.5 N was applied with a driving voltage of 13 V to the piezoelectric actuator. The right tibia was used as nonloading control. After loading the mouse was allowed a normal cage activity, and any abnormal behavior, a weight loss, or a diminished food intake was monitored.

Measurements with strain gauge. Four mice were used for the measurements. Loads with the knee-loading modality were confined near the loading site, and no bending moment was presumably generated to the tibia or the femur. To evaluate in situ strains at the site of histomorphometric analyses in the tibia, strain measurements were conducted using the procedure previously described (6, 18) (Fig. 2). The mouse was killed, and the medial periosteal surface of a left tibia was exposed and cleared. A strain gauge of a single element type with 0.7 mm in width and 2.8 mm in length (model EA-06-015DJ-120, Measurements Group) was then glued to the medial periosteal surface 25% (~4 mm) distant from the proximal end of the tibia. Because a part of tissues was removed from the tibia to place the strain gauge, we recalibrated force applied to the leg with the strain gauge. The deflection of the cantilever was used to estimate the applied force to the leg with and without the strain gauge. A partial removal of tissues for attaching the strain gauge was statistically insignificant to alter the applied force to the knee. The knee was loaded at 2, 5, 10, and 15 Hz with 0.5-, 1-, and 2-N forces (peak to peak) in the lateral-medial direction. Voltage signals from the strain gauge were sent to the computer via a signal conditioning amplifier (2210, Measurement Group), and Fourier transform was applied to remove the noise from the signal. The measurement was repeated five times, and the peak-to-peak voltage was converted to the actual strain value by using the standard calibration line.

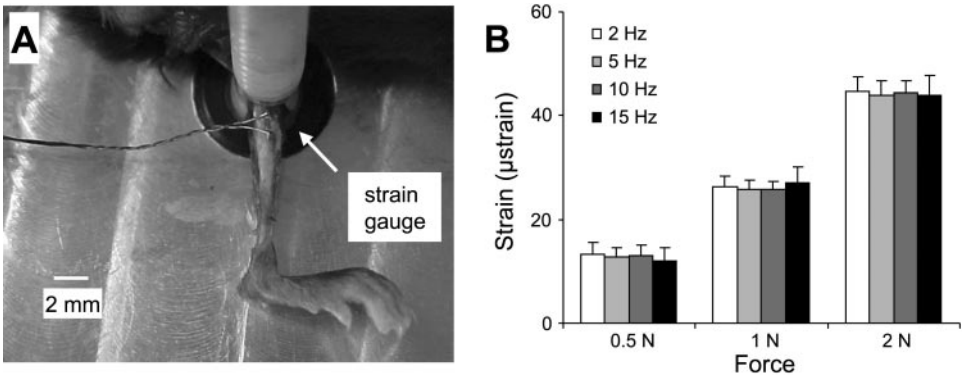

Fig. 2. Strains induced in knee loading. *A*: strain gauge attached to the tibia. Scale bar is 2 mm. *B*: measured strains in response to loads of 0.5-, 1-, and 2-N forces applied to the knee with the loading frequency at 2, 5, 10, and 15 Hz. Results are expressed as means ± SE.

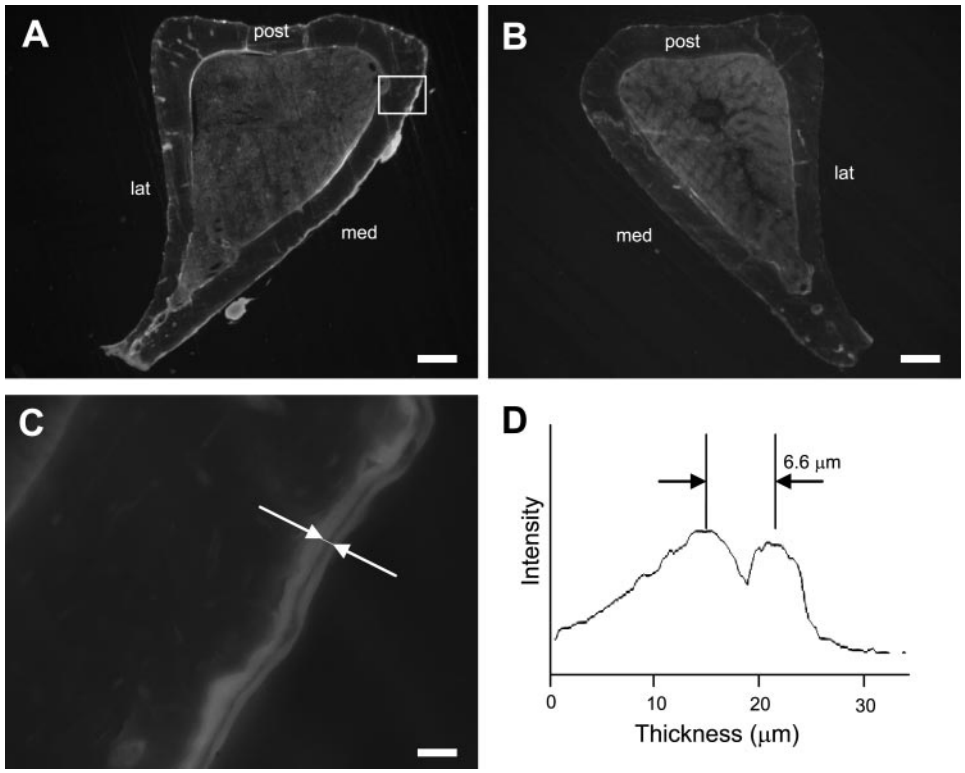

Fig. 3. Tibial sections with and without knee loading. *A*: cross section of the loaded tibia with 0.5-N force at 5 Hz. The section was obtained ~4 mm distant from the proximal end of the tibia. Labels are medial (med), lateral (lat), and posterior (post) surfaces. White bar is 200 μm. *B*: cross section of control tibia (no loading). *C*: double-labeled periosteal surface of the loaded tibia. Bright lines represent fluorescent calcein strips. White bar is 20 μm. *D*: fluorescence intensity along the line indicated in *C*. The distance between 2 lines, 6.6 μm in the diagram, indicates the newly formed bone in 4 days.

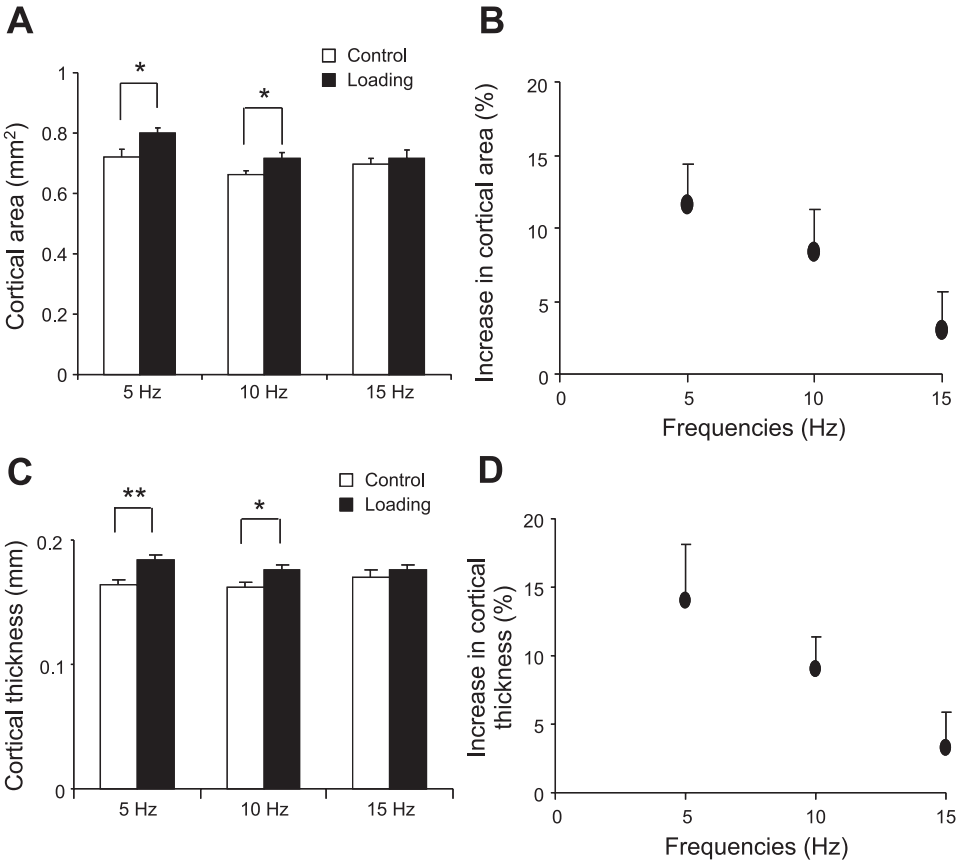

Fig. 4. Alteration in cross-sectional area and cortical thickness with the knee loading at 5, 10, and 15 Hz. Results are expressed as means ± SE. $*P < 0.05$; $**P < 0.01$. *A*: cross-sectional area (mm^2). *B*: increase in cross-sectional area (% of control). *C*: cortical thickness (mm). *D*: increase in cortical thickness (% of control).

Bone histomorphometry. Mice were given an intraperitoneal injection of calcein (Sigma, St. Louis, MO), a fluorochrome bone label, at 30 μg/g body mass on *days 2* and *6* after the last loading. Animals were killed 13 days after the last loading, and the left and right tibiae were harvested for bone histomorphometry. The isolated bones were cleaned of soft tissues, and the distal and the proximal ends were cleaved to allow infiltration of fixatives. Specimens were dehydrated in a series of graded alcohols and embedded in methyl methacrylate (Aldrich Chemical, Milwaukee, WI). The transverse sections (~80 μm in thickness) were removed from the region 25% distant from the proximal ends of the tibiae by using a diamond-embedded wire saw (Delaware Diamond Knives, Wilmington, DE), and they were mounted on standard microscope slides (Fig. 3).

The histomorphometrical data were collected from the periosteal and endosteal surfaces of the tibia. The periosteal surface was divided into the medial surface, the lateral surface, and the posterior surface (2). By use of a Nikon Optiphot fluorescence microscope (Nikon, Garden City, NY) and a Bioquant digitizing system (R & M Biometrics, Nashville, TN), the morphometric data were collected. Measurements included periosteal and endocortical perimeter (B.Pm), total bone sectional area, sectional area of bone marrow cavity, single-labeled perimeter (sL.Pm), double-labeled perimeter (dL.Pm), and double-labeled area (dL.Ar). From these measurements, the following quantities were derived: mineralizing surface [MS/BS; = (1/2 sL.Pm + dL.Pm)/B.Pm, in %], mineral apposition rate (MAR; = $dL.Ar \cdot dL.Pm^{-1} \cdot 4^{-1}$, in μm/day), and bone formation rate (BFR/BS; = MAR × MS/BS × 365 in $\mu m^3 \cdot \mu m^{-2} \cdot yr^{-1}$). In drawing a fluorescent intensity curve, MetaMorph Imaging System (version 3.6, Universal Imaging) was used.

To examine load-driven alteration in bone size, the cortical bone area was determined by subtracting the cross-sectional area of bone marrow cavity from the total bone sectional area. The cortical thickness was also defined as mean distance between the endosteal and the periosteal surfaces on the three sides (medial, lateral, and posterior). The measurements were taken in the middle of each side, and the mean value was calculated from three independent measurements. The normalized alteration in the cross-sectional cortical area and the cortical thickness was determined as differences between left (L; loaded) and right (R; control) tibias such as [(L − R)/R × 100 in %]. To evaluate the effects of the loading frequencies, the relative parameters such as rMS/BS, rMAR, and rBFR/BS were derived. These relative parameters were calculated as differences of the values in the loaded tibia from those in the control tibia.

Statistical analysis. The data were expressed as means ± SE. Statistical significance among groups was examined by ANOVA, and a post hoc test was conducted using a Fisher's protected least significant difference test. A paired *t*-test was employed to evaluate statistical significance between the loaded and control samples. All comparisons were two-tailed, and $P < 0.05$ was assumed for the level of statistical significance.

RESULTS

The animals used for bone histomorphometry tolerated the procedures, and any abnormal behavior including weight loss and diminished food intake was not observed. No bruising or other damages were detected at the loading site.

Strain measurements with the knee-loading modality. In response to the loads with the knee-loading modality, the strain in the tibial diaphysis, 25% (~4 mm) distant from the proximal end along the length of the tibia, was measured. It is unavoidable to remove a part of tissues from the tibia for attaching the strain gauge. To evaluate any effect of this tissue removal on

Table 1. *Bone formation in periosteum and endosteum at the loading frequencies of 5, 10, and 15 Hz*

	MS/BS, %	*P* Value	MAR, μm/day	*P* Value	BFR/BS, $\mu m^3 \cdot \mu m^{-2} \cdot yr^{-1}$	*P* Value
			5 Hz			
Periosteum						
Control	17.62±73		0.38±0.02		23.69±.9	
Knee loading	26.23±65		0.65±0.02		61.49±.54	
	1.5 ×	<0.01	1.7 ×	<0.001	2.6 ×	<0.001
Endosteum						
Control	22.25±77		0.41±0.06		35.55±7.04	
Knee loading	31.1±25		0.55±0.04		61.79±10.09	
	1.4 ×	NS	1.3 ×	NS	1.7 ×	NS
			10 Hz			
Periosteum						
Control	13.26±0.95		0.33±0.01		15.85±1.29	
Knee loading	19.12±1.18		0.46±0.04		32.82±4.78	
	1.4 ×	<0.05	1.4 ×	<0.01	2.1 ×	<0.01
Endosteum						
Control	10.40±1.41		0.34±0.03		13.21±2.16	
Knee loading	15.00±4.11		0.42±0.03		24.34±8.24	
	1.4 ×	NS	1.2 ×	NS	1.8 ×	NS
			15 Hz			
Periosteum						
Control	16.42±3.76		0.34±0.02		21.36±5.64	
Knee loading	19.73±2.09		0.37±0.02		26.89±3.66	
	1.2 ×	NS	1.1 ×	NS	1.3 ×	NS
Endosteum						
Control	19.2±4.59		0.32±0.04		25.16±8.29	
Knee loading	24.54±3.89		0.39±0.03		37.03±6.8	
	1.3 ×	NS	1.2 ×	NS	1.5 ×	NS

Values are means ± SE. MS/BS, mineralizing surface; MAR, mineral apposition rate; BFR/BS, bone formation rate. NS indicates that the *P* value exceeds 0.05.

the force applied to the knee, we recalibrated the driving voltage to the piezoelectric actuator. Compared with the load to the intact leg, the loads applied to the leg lacking a part of skin and connective tissues were measured ~8% higher although no statistical significance was observed (data not shown) in the presence of the background noise of ~10 μstrain. ANOVA was conducted among the loading frequencies of 2, 5, 10, and 15 Hz in response to the loads of 0.5 N ($P = 0.97$), 1 N ($P = 0.97$), and 2 N ($P = 0.99$), and the results showed no clear dependence of the measured strain on the loading frequencies (Fig. 2*B*). Hereafter, we used 0.5 N as the loads for our analysis of osteogenic potentials in the tibial diaphysis. Note that the loads would not induce detectable in situ strain with the knee loading in the region of investigation in the present study.

Load-driven alteration in cortical area and thickness. The applied loads increased the cross-sectional area and the cortical thickness of the loaded tibia, and the enhancement was dependent on the loading frequencies (Fig. 4). The cross-sectional cortical area increased by 11% at 5 Hz ($P < 0.05$) and 8% at 10 Hz ($p < 0.05$). No significant alteration was observed at 15 Hz ($P = 0.55$). The cortical thickness increased from 0.165 ± 0.004 mm (control) to 0.185 ± 0.004 mm (loading) at 5 Hz ($P < 0.01$) and from 0.163 ± 0.004 mm (control) to 0.176 ± 0.004 mm (loading) at 10 Hz ($P < 0.05$). No significant changes were observed at 15 Hz ($P = 0.49$). The percent change in the cross-sectional cortical area and the cortical thickness among the three loading frequencies was compared. There was no statistical difference among the three loading frequencies, although the increase in cortical area ($P = 0.12$) and thickness ($P = 0.06$) approached statistical significance.

Bone formation in periosteum and endosteum. Bone formation on the periosteal surface was stimulated by the knee-loading modality at 5 Hz and 10 Hz (Table 1). Compared with the nonloading control, loading at 5 Hz resulted in a significant increase in three morphometric parameters (1.5× for MS/BS with $P < 0.01$, 1.7× for MAR with $P < 0.001$, and 2.6× for BFR/BS with $P < 0.001$). Similarly, the loading at 10 Hz elevated these parameters (1.4 × for MS/BS with $P < 0.05$, 1.4 × for MAR with $P < 0.01$, and 2.1 × for BFR/BS with $P < 0.01$). No statistical difference was observed by the loading at 15 Hz ($P = 0.65$–0.71).

Dependence on the loading frequencies was also observed in the relative parameters defined on the periosteal surface (Fig. 5). The value of rMAR was significantly increased by the loading at 5 Hz ($P < 0.01$ to 10 Hz; $P < 0.001$ to 15 Hz), and it was larger at 10 Hz than at 15 Hz ($P < 0.05$). Likewise, the value of rBFR/BS was largest with the loading at 5 Hz ($P < 0.01$ to 10 Hz; $P < 0.001$ to 15 Hz). Note that there were no statistical differences in rMS/BS among the three loading frequencies ($P = 0.30$).

To further evaluate the effects of knee loading on the periosteal and endosteal surfaces, an increase in rMS/BS, rMAR, and rBFR/BS was obtained. In the increase on the periosteal surface normalized by the control value, the loading at 5 Hz elevated rMAR ($P < 0.001$) and rBFR/BS ($P < 0.01$) more than the loading at 15 Hz. Unlike the periosteal surface, no significant loading effects were observed on the endosteal surface at any loading frequencies ($P = 0.51$–0.98; data not shown).

Comparison among the medial, lateral, and posterior surfaces in periosteum. The knee-loading modality had differential effects on three periosteal surfaces (Table 2). The loading at 5 Hz increased the morphometric parameters on the medial surface (1.6 × for MS/BS with $P < 0.01$, 2.0 × for MAR with $P < 0.001$, and 3.3 × for BFR/BS with $P < 0.001$) and the lateral surface (1.4 × for MS/BS with $P < 0.05$, 1.4 × for MAR with $P < 0.01$, and 1.9 × for BFR/BS with $P < 0.001$). In comparison, the loading at 10 Hz enhanced bone formation on the medial surface only (1.6 × for MS/BS with $P < 0.05$, 1.6 × for MAR with $P < 0.01$, and 2.5 × for BFR/BS with $P < 0.01$). No significant loading effect was observed at 15 Hz ($P = 0.17$–0.66).

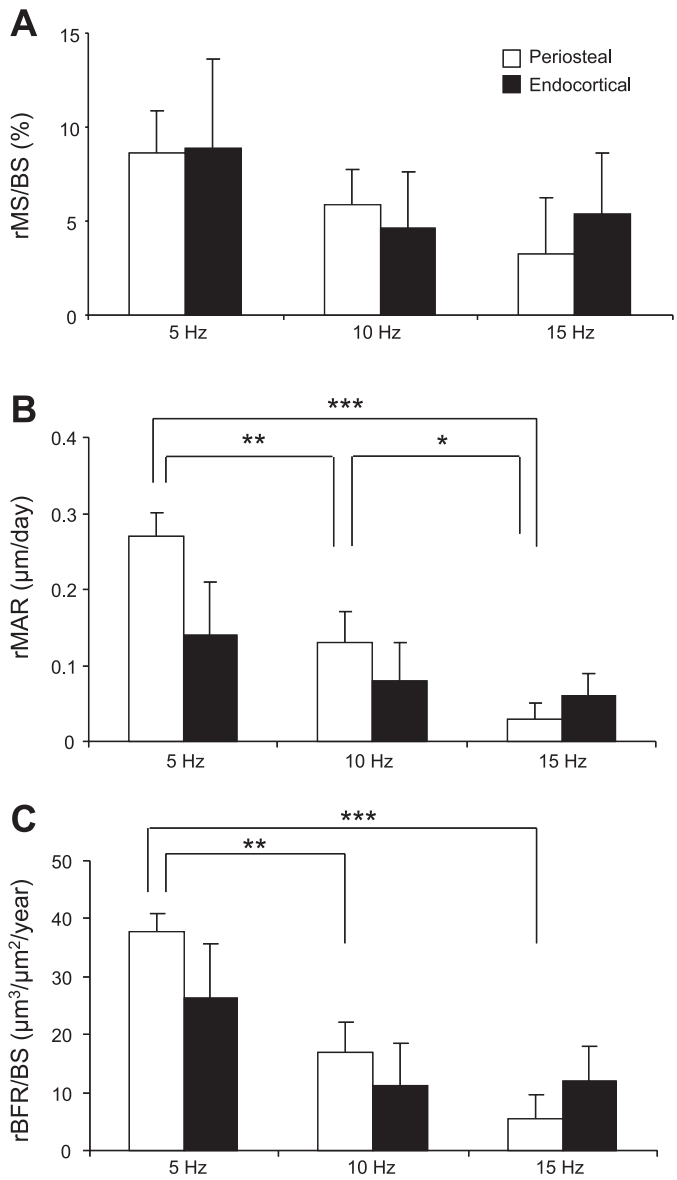

Fig. 5. Alteration in the histomorphometric parameters on the periosteal and endosteal surfaces with knee loading at 5, 10, and 15 Hz. Results are expressed as means ± SE. *$P < 0.05$, **$P < 0.01$, ***$P < 0.001$, based on Fisher's protected least significant difference at $\alpha = 0.05$. *A*: relative mineralizing surface (rMS/BS; %). *B*: relative mineral apposition rate (rMAR; μm/day). *C*: relative bone formation rate (rBFR/BS; $\mu m^3 \cdot \mu m^{-2} \cdot yr^{-1}$).

Table 2. *Bone formation on medial, lateral, and posterior surfaces at loading frequencies of 5, 10, and 15 Hz*

	MS/BS, %	*P* Value	MAR, μm/day	*P* Value	BFR/BS, $\mu m^3 \cdot \mu m^{-2} \cdot yr^{-1}$	*P* Value
			5 Hz			
Medial						
Control	20.3±2.39		0.39±0.04		28.6±4.28	
Knee loading	33.49±2.53		0.78±0.03		94.23±5.22	
	1.6 ×	<0.01	2.0 ×	<0.001	3.3 ×	<0.001
Lateral						
Control	15.29±1.52		0.39±0.02		21.34±1.79	
Knee loading	21.23±2.23		0.53±0.04		40.16±4.13	
	1.4 ×	<0.05	1.4 ×	<0.01	1.9 ×	<0.001
Posterior						
Control	16.61±2.47		0.32±0.03		18.82±2.82	
Knee loading	21.14±3.24		0.42±0.06		34.68±9.96	
	1.3 ×	NS	1.3 ×	NS	1.8 ×	NS
			10 Hz			
Medial						
Control	15.58±1.25		0.34±0.02		19.63±2.08	
Knee loading	24.48±2.8		0.54±0.06		48.87±7.35	
	1.6 ×	<0.05	1.6 ×	<0.01	2.5 ×	<0.01
Lateral						
Control	11.84±1.32		0.32±0.02		14.03±2.06	
Knee loading	16.15±2.58		0.39±0.03		24.27±4.6	
	1.4 ×	NS	1.2 ×	NS	1.7 ×	NS
Posterior						
Control	11.17±1.21		0.30±0.01		12.37±1.64	
Knee loading	13.86±1.65		0.35±0.02		17.46±2.03	
	1.2 ×	NS	1.2 ×	NS	1.4 ×	NS
			15 Hz			
Medial						
Control	17.31±4.94		0.38±0.05		24.78±8.24	
Knee loading	21.76±2.73		0.42±0.03		32.19±3.32	
	1.3 ×	NS	1.1 ×	NS	1.3 ×	NS
Lateral						
Control	16.12±3.75		0.31±0.03		19.72±5.61	
Knee loading	18.16±2.5		0.34±0.04		24.44±5.74	
	1.1 ×	NS	1.1 ×	NS	1.2 ×	NS
Posterior						
Nonloaded	15.45±2.31		0.28±0.03		16.48±3.56	
Loaded	18.19±2.14		0.33±0.03		21.52±2.55	
	1.2 ×	NS	1.2 ×	NS	1.3 ×	NS

Values are means ± SE. NS indicates the *P* value exceeds 0.05.

Enhancement of the relative bone morphometric parameters on the medial surface in periosteum was dependent on the loading frequencies (Fig. 6). The frequency at 5 Hz resulted in a significant increase in both rMAR ($P < 0.01$ to 10 Hz; $P < 0.001$ to 15 Hz) and rBFR/BS (both $P < 0.001$ to 10 and 15 Hz). The change in rMAR and rBFR/BS was significantly higher at 10 Hz than 15 Hz ($P < 0.05$). Note that there were no statistical differences in rMS/BS among the three loading frequencies ($P = 0.23$).

To further evaluate the effects of knee loading on the three periosteal surfaces, the percent change in bone formation on the periosteal medial, lateral, and posterior surfaces was determined. In the normalized change in the medial surface, the loading at 5 Hz resulted in significantly greater rMAR than the loading at 15 Hz ($P < 0.01$). Note that there were no statistical differences in rMS/BS among the three loading frequencies ($P = 0.85$). There was no statistical difference among the three loading frequencies in rBFR/BS, although the increase approached to statistical significance ($P = 0.07$).

DISCUSSION

The present study investigated the osteogenic effect of loads applied to the proximal epiphysis of the tibia. The applied force of 0.5 N is significantly smaller than the required force of 2 N or more in the axial loading modality with mouse ulnae (33). The results clearly demonstrate that the knee-loading modality is able to enhance bone formation on the periosteal surface of the tibia, which is located ~4 mm distal to the loading site. Many animal studies on load-induced bone remodeling indicate that bone formation is driven by dynamic loading, and load-induced strain is a principal determinant (10, 29). Although in situ strains above the minimum effective strain value at 1,000–2,000 μstrain are often considered a threshold to stimulate load-driven formation (19, 27, 33), our measured strain at the site of bone formation was two orders of magnitude smaller than the threshold and in the same order of magnitude as the measurement noise at ~10 μstrain. High-frequency vibration at 30 Hz was reported to strengthen trabecular bones with <10 μstrain (20, 22), and therefore the

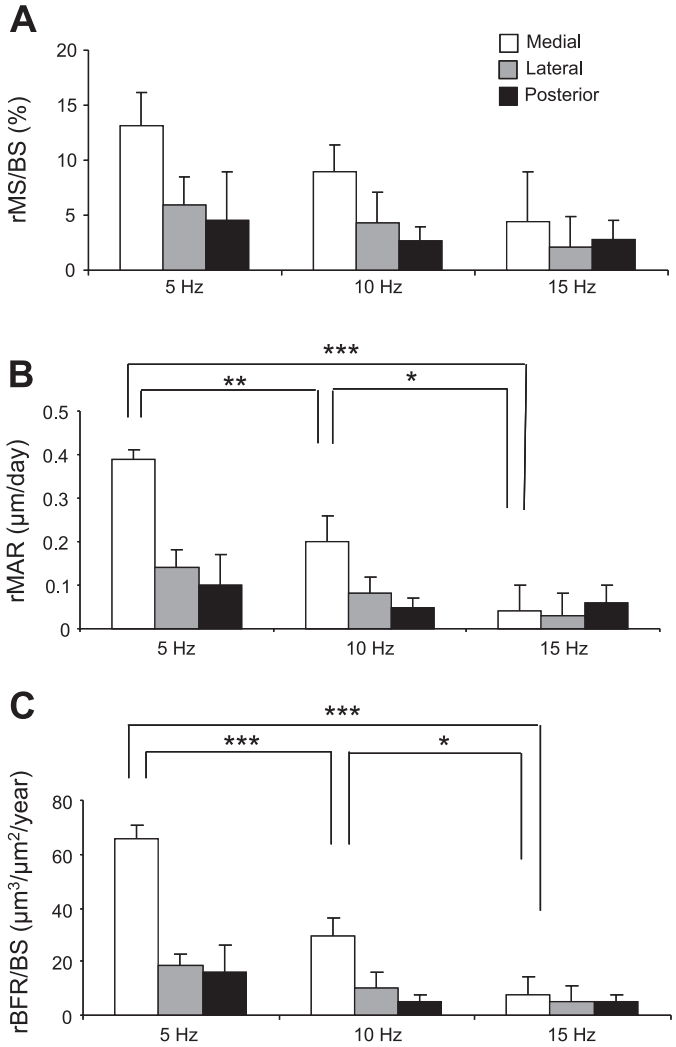

Fig. 6. Medial, lateral, and posterior surfaces with the knee loading at 5, 10, and 15 Hz. Results are expressed as means ± SE. $*P < 0.05$, $**P < 0.01$, $***P < 0.001$, based on Fisher's protected least significant difference at $\alpha = 0.05$. *A*: rMS/BS (%). *B*: rMAR (μm/day). *C*: rBFR/BS ($\mu m^3 \cdot \mu m^{-2} \cdot yr^{-1}$).

present study presents another loading method that requires virtually no in situ strain. Note that the measured strain in ulnar cortical bone with the elbow-loading modality was also in the order of 10 μstrain (34). The number of daily loading cycles with knee loading in the present study was 900–2,700, which was approximately two orders of magnitude smaller than the required daily loading cycles with whole body vibrations (21). Taken together, the results strongly suggest that bone formation can be achieved with no virtual in situ strain in cortical bone with the joint-loading modality.

The present study focused on diaphyseal cortical bone distant from the loading site in the proximal epiphysis, and we observed differential sensitivity of the periosteal and endosteal surfaces to the applied loads. In contrast to the marked enhancement of bone formation in the periosteal surface, the endosteal surface showed no significant increase in any of the three bone morphological parameters. Furthermore, the three periosteal surfaces responded differently and sensitivity to the loading was highest on the medial surface and lowest on the posterior surface. Because the loading was applied in the lateral-medial direction on the periosteal surface, the results suggest that the mechanical configuration at the loading site in the epiphysis influences enhancement of bone formation in the diaphysis distant from the loading site.

The precise mechanism for the observed anabolic effects in this study is unclear and merits future investigation. A conceivable hypothesis underlying these observations of bone formation with the knee-loading modality is that mechanical loads applied to the epiphysis induce the osteogenic signal towards the diaphysis through fluid flow in the lacunocanalicular network (1st model) or through alteration in blood circulation (2nd model) (Fig. 7). In the first model, the direct signal is shear stress and/or augmented molecular transport with a gradient of intramedullary pressure, which is driven in the loaded epiphysis and conducted to the nonloaded diaphysis (3, 12, 13, 24). In the second model, the signal is elevated through altered blood circulation at the loading site and its subsequent propagation to the site of bone formation (31, 32). Fluid flow by in situ strain is proposed to explain enhancement of bone formation with the axial loading modality, but in our first model fluid flow is originated at the loading site, which is remotely located from the site of bone formation. The mechanism of flow induction may include convection in the lacunocanalicular network and pressure alteration in an intramedullary cavity. As suggested by Qin et al. (16) with their elegant pressure experiment, it is conceivable that intramedullary pressure and differential microstructure of bone on differing surfaces may dictate the spatial nonuniformity of the observed anabolic responses. The second model is considered as a mechanism for bone formation with femoral vein ligation (1). Other factors such as induction of electrochemical streaming potentials (17) and muscle contraction (31) can be involved, and further analyses beyond bone histomorphometry will be necessary to examine the above hypotheses.

It has been known that efficacy of load-driven bone formation is affected by loading frequencies (26, 28, 33). In our limited frequency analysis, the loading frequency at 5 Hz was

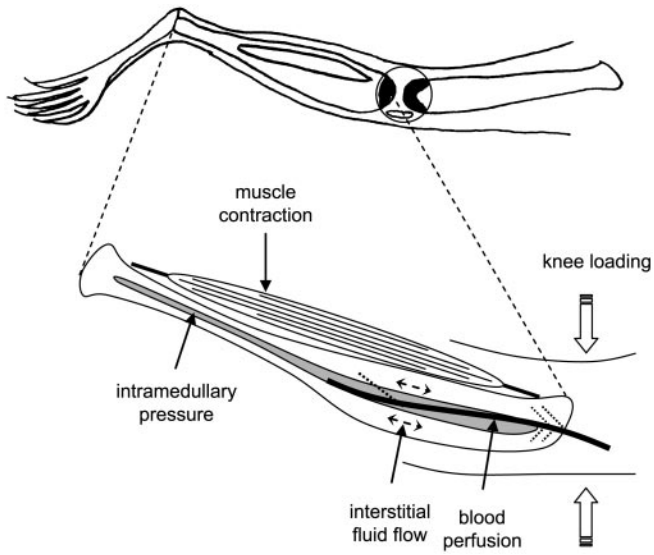

Fig. 7. Potential contributors to enhance bone formation in the tibia with knee loading. This schematic illustration includes muscle contraction, alteration in intramedullary pressure, load-driven interstitial fluid flow, and activation of blood perfusion.

most effective among the 5, 10, and 15 Hz (35). The ulna-loading modality is shown to enhance bone formation with an increase in the loading frequencies from 1 to 10 Hz (7), and the loading at 5 and 10 Hz had higher osteogenic potentials than that at 20 or 30 Hz (33). In low-level high-frequency vibrations, on the other hand, it is suggested that higher frequencies can stimulate bone formation with a lower level of vibration (20, 22). Bone cells may alter cellular stiffness in a frequency-dependent fashion (4, 8) and change their sensitivity to load-driven interstitial fluid flow or muscle contraction. Alternatively, induction of interstitial fluid flow in lacunocanalicular networks or activation of muscle contraction might be affected by loading frequencies.

In summary, we demonstrate that the knee-loading modality is an effective means to enhance bone formation in the tibial periosteal surface with virtually no strain at the site of bone formation. Efficacy of the modality depends on the loading frequency, and the maximum bone formation is achieved by the loading at 5 Hz. These results extend our knowledge on the interplay between bone and joints and potentially provide a novel therapeutic treatment to strengthening bone.

ACKNOWLEDGMENTS

The authors appreciate Dr. G. M. Malacinski for critical reading of the manuscript.

GRANTS

This study was in part supported by National Institute on Aging Grant AG-024596. The authors have no conflict of interest.

REFERENCES

1. **Bergula AP, Huang W, and Frangos JA.** Femoral vein ligation increases bone mass in the hindlimb suspended rat. *Bone* 24: 171–177, 1999.
2. **Burger EH and Klein-Nulend J.** Mechanotransduction in bone-role of the lacuno-canalicular network. *FASEB J* 13: S101–S112, 1999.
3. **Burr DB, Robling AG, and Turner CH.** Effects of biomechanical stress on bones in animals. *Bone* 30: 781–786, 2002.
4. **Donahue SW, Jacobs CR, and Donahue HJ.** Flow-induced calcium oscillations in rat osteoblasts are age, loading frequency, and shear stress dependent. *Am J Physiol Cell Physiol* 281: C1635–C1641, 2001.
5. **Forwood MR and Turner CH.** Skeletal adaptations to mechanical usage: results from tibial loading studies in rats. *Bone* 17: 197S–205S, 1995.
6. **Hsieh YF, Robling AG, Ambrosius WT, Burr DB, and Turner CH.** Mechanical loading of diaphyseal bone in vivo: the strain threshold for an osteogenic response varies with location. *J Bone Miner Res* 16: 2291–2297, 2001.
7. **Hsieh YF and Turner CH.** Effects of loading frequency on mechanically induced bone formation. *J Bone Miner Res* 16: 918–924, 2001.
8. **Jacobs CR, Yellowley CE, Davis BR, Zhou Z, Cimbala JM, and Donahue HJ.** Differential effect of steady vs oscillating flow on bone cells. *J Biomech* 31: 969–976, 1998.
9. **Jiang H, Liu Y, Wang E, and Yokota H.** Development of a mechanical loader to evaluate load-driven molecular transport. *Proc 51st Annual ORS Meeting 2004*, p. 145.
10. **Judex S, Gross TS, and Zernicke RF.** Strain gradients correlate with sites of exercise-induced bone-forming surfaces in the adult skeleton. *J Bone Miner Res* 12: 1737–1745, 1997.
11. **Kameyama Y, Hagino H, Okano T, Enokida M, Fukata S, and Teshima R.** Bone response to mechanical loading in adult rats with collagen-induced arthritis. *Bone* 35: 948–956, 2004.
12. **Knothe Tate ML and Knothe U.** An ex vivo model to study transport processes and fluid flow in loaded bone. *J Biomech* 33: 247–254, 2000.
13. **Montgomery RJ, Sutker BD, Bronk JT, Smith SR, and Kelly PJ.** Interstitial fluid flow in cortical bone. *Microvasc Res* 35: 295–307, 1988.
14. **Patel RB, O'Leary JM, Bhatt SJ, Vasnja A, and Knothe Tate ML.** Determining the permeability of cortical bone at multiple length scales using fluorescence recovery after photobleaching techniques. *Proc 51st Annual ORS Meeting 2004*, p. 141.
15. **Pedersen EA, Akhter MP, Cullen DM, Kimmel DB, and Recker RR.** Bone response to in vivo mechanical loading in C3H/HeJ mice. *Calcif Tissue Int* 65: 41–46, 1999.
16. **Qin YX, Kaplan T, Saldanha A, Rubin CT.** Fluid pressure gradients, arising from oscillations in intramedullary pressure, is correlated with the formation of bone and inhibition of intracortical porosity. *J Biomech* 36: 1427–1437, 2003.
17. **Qin YX, Lin W, and Rubin CT.** The pathway of bone fluid flow as defined by in vivo intramedullary pressure and streaming potential measurements. *Ann Biomed Eng* 30: 693–702, 2002.
18. **Robling AG and Turner CH.** Mechanotransduction in bone: genetic effects on mechanosensitivity in mice. *Bone* 31: 562–569, 2002.
19. **Rubin CT and Lanyon LE.** Regulation of bone mass by mechanical strain magnitude. *Calcif Tissue Int* 37: 411–417, 1985.
20. **Rubin CT, Recker R, Cullen D, Ryaby J, McCabe J, and McLeod K.** Prevention of postmenopausal bone loss by a low-magnitude, high-frequency mechanical stimuli: a clinical trial assessing compliance, efficacy, and safety. *J Bone Miner Res* 19: 343–351, 2004.
21. **Rubin CT, Sommerfeldt DW, Judex S, Qin Y.** Inhibition of osteopenia by low magnitude, high-frequency mechanical stimuli. *Drug Discov Today* 15: 848–858.
22. **Rubin CT, Turner AS, Bain S, Mallinckrodt C, and McLeod K.** Anabolism. Low mechanical signals strengthen long bones. *Nature* 412: 603–604, 2001.
23. **Su M, Zhang P, Cheng T, and Yokota H.** Load-driven molecular transport in response to knee loading. *Proc 52nd Annual ORS Meeting 2006*, p. 1027.
24. **Tami AE, Nasser P, Verborgt O, Schaffler MB, and Knothe Tate ML.** The role of interstitial fluid flow in the remodeling response to fatigue loading. *J Bone Miner Res* 17: 2030–2037, 2002.
25. **Tanaka SM, Sun HB, and Yokota H.** Bone formation induced by a novel form of mechanical loading on joint tissue. *Biol Sci Space* 18: 41–44, 2004.
26. **Turner CH, Forwood MR, and Otter MW.** Mechanotransduction in bone: do bone cells act as sensors of fluid flow? *FASEB J* 8: 875–878, 1994.
27. **Turner CH, Forwood MR, Rho JY, and Yoshikawa T.** Mechanical loading thresholds for lamellar and woven bone formation. *J Bone Miner Res* 9: 87–97, 1994.
28. **Turner CH, Owan I, and Takano Y.** Mechanotransduction in bone: role of strain rate. *Am J Physiol Endocrinol Metab* 269: E438–E442, 1995.
29. **Turner CH.** Three rules for bone adaptation to mechanical stimuli. *Bone* 23: 399–407, 1998.
30. **Wang L, Ciani C, Doty SB, and Fritton SP.** Delineating bone's interstitial fluid pathway in vivo. *Bone* 34: 499–509, 2004.
31. **Wang L, Fritton SP, Weinbaum S, and Cowin SC.** On bone adaptation due to venous stasis. *J Biomech* 36:1439–1451, 2003.
32. **Wang L, Henderson SC, Majeska RJ, and Schaffler MB.** In situ measurement of molecular diffusion in the osteocyte lacunar-canalicular system of intact bone. *Proc 50th Annual ORS Meeting 2003,* p. 327.
33. **Warden SJ and Turner CH.** Mechanotransduction in cortical bone is most efficient at loading frequencies of 5–10 Hz. *Bone* 34: 261–270, 2004.
34. **Yokota H and Tanaka SM.** Osteogenic potential with joint loading modality. *J Bone Miner Metab* 23: 302–308, 2005.
35. **Zhang P, Su M, Cheng T, and Yokota H.** Femoral bone formation response to knee loading. *Proc 52nd Annual ORS Meeting* 1754, 2006.